Registry No. *trans*-[Co(3,2,3-tet)$(NH_3)_2$]Cl_3, 81120-92-5; *trans*-[Co(2,3,2-tet)$(NH_3)_2$]Cl_3, 81120-93-6; *trans*-[Co(3,2,3-tet)$(N_3)_2$]BF_4, 81120-95-8; *trans*-[Co(3,2,3-tet)Cl_2]Cl, 31842-33-8; *trans*-[Co(2,3,2-tet)Cl_2]Cl, 15041-27-7; *trans*-[Co(3,2,3-tet)$Br_2]^+$, 55722-17-3; *trans*-[Co(3,2,3-tet)$(OAc)_2]^+$, 47100-49-2; *trans*-[Co(3,2,3-tet)$(NO_2)_2]^+$, 55722-18-4; *trans*-[Co(2,3,2-tet)$(gly)_2]^+$, 81244-25-9; *trans*-[Co(2,3,2-tet)$(OAc)_2]^+$, 57022-13-9; *trans*-[Co(2,3,2-tet)$(NO_2)_2]^+$, 46845-89-0.

Contribution from the Departments of Chemistry, Texas A&M University, College Station, Texas 77843, and University of Antwerp (U.I.A.), B-2610 Wilrijk, Belgium

Synthesis and Spectroscopic Properties of Divalent and Trivalent Tris(2,2'-bipyridine)iron Complexes in Zeolite Y

WILLIAM H. QUAYLE,[1] GUIDO PEETERS,[2] GILBERT L. DE ROY,[2] ETIENNE F. VANSANT,[2] and JACK H. LUNSFORD*[1]

Received July 13, 1981

Mössbauer, EPR, and visible-region diffuse-reflectance techniques were used to characterize divalent and trivalent tris-(2,2'-bipyridine)iron complexes which had been synthesized within the large cavities of Y-type zeolites at low and high loadings. Exposure of samples containing the divalent Fe complex to chlorine gas produced the supported trivalent complex. The spectroscopic data for the low-loading iron complexes in the zeolite were similar to data obtained for $Fe(bpy)_3$ complexes in other matrices; i.e., for $[Fe^{II}(bpy)_3]$-Y(5.3) λ_{max} = 528, 495, and 353 nm, IS = 0.626, and QS = 0.339 mm/s and for $[Fe^{III}(bpy)_3]$-Y(5.3) λ_{max} = 612 nm, $g_\perp = -2.60 \pm 0.02$, and $g_\parallel = 1.66 \pm 0.01$. Differences were attributed to the probable higher negative charge density within the zeolite. The bipyridine ligand complexed 88% of the iron specifically in the tris form, and chlorine gas oxidized 89% of this divalent complex. With the high-loading sample, only 55% of the total iron was complexed by bipyridine since the iron content exceeded that necessary for one large tris complex per supercage. Excess Fe(II) was apparently close enough that it exerted an electron-withdrawing influence on the bpy ligands. Only 33% of the bpy complexes were effectively oxidized by chlorine gas, presumably due to exclusion of Cl_2 or Cl^- from certain cation sites.

Introduction

Well-characterized transition-metal complexes such as $[Cu(en)_2]^{2+}$ [3] synthesized within a zeolite, either by direct ion exchange of the complex or sorption of the ligand within the support, serve as models of complex-support interactions which may occur during photochemical or catalytic reactions. We recently examined the spectroscopic and redox properties of large tris(2,2'-bipyridine)ruthenium(II) and -(III) complexes located in supercages of Y-type zeolites.[4,5] The photophysical behavior of the ruthenium(II) complex in the zeolite was altered from that commonly observed for the solution phase complex in ways that could be rationalized in terms of synergistic complex-support interplay.[4] Since the zeolite offered a regular, characterizable medium in which potential nonaqueous, aqueous, or gas-phase photochemistry could be conducted, we initiated studies designed to test the thermal and photo activities for reactions of small molecules within these materials. As part of that study the chlorine oxidation of $[Ru^{II}(bpy)_3]^{2+}$ ions in a Y-type zeolite was undertaken in order to evaluate the thermal reaction of the respective trivalent complex with water.[5]

This report describes the spectroscopic properties of divalent and trivalent iron tris(bipyridine) complexes in zeolite Y. Since the diameter of the $[Fe^{II}(bpy)_3]^{2+}$ complexes was too large ($\sim$1 nm) to exchange directly through the zeolite lattice free apertures ($\sim$0.74 nm),[6] a procedure for in situ synthesis of the complex was adopted.

Experimental Section

$[Fe^{II}(bpy)_3]$-Y. A $[Fe^{II}(bpy)_3]$-Y(5.3) sample which contained 1.7 wt % Fe or 5.3 Fe ions per unit cell was prepared by exchange of 8.00 g of Na-Y zeolite (Linde) with 1.00 g of $Fe^{II}SO_4 \cdot 7H_2O$ (Fisher) in an aqueous solution, pH 4, under flowing N_2. The Fe^{II}-Y zeolite was then washed and dried at room temperature. A 4.00-g sample of the Fe^{II}-Y zeolite was mixed with 1.00 g of 2,2'-bipyridine, degassed for 4 h at 25 °C, and then heated at 200 °C overnight in a closed system. The preparative mole ratio of Fe to bpy was about 1:3.5. The reddish pink product was subsequently degassed at 200 °C to 5×10^{-4} torr.

A Fe^{II}-Y sample used for the synthesis of the higher loading $[Fe^{II}(bpy)_3]$-Y(13) sample which contained 4.0 wt % Fe or 13 Fe ions per unit cell was prepared after the method of Delgass et al.[7] by exchange of 5 g of Na-Y with an excess (12.2 g) of $Fe^{II}SO_4 \cdot 7H_2O$ in a pH 4 solution under N_2. The reaction with bpy was analogous to the low-loading preparation except that 0.33 g of bpy/g of zeolite was used to produce the deep red product.

An impregnated $[Fe^{II}(bpy)_3]$-Y sample was prepared by addition of bpy in about a 3:1 bpy:Fe mole ratio to an $Fe^{II}(aq)$ solution. This produced $[Fe^{II}(bpy)_3]^{2+}$, to which some Na-Y was added with stirring. Filtration and drying at room temperature yielded a light pink material.

$[Fe^{III}(bpy)_3]$-Y. A 1-g sample of $[Fe^{II}(bpy)_3]$-Y(5.3) was placed in a sample tube equipped with a 0.5-cm fused quartz curvette, for diffuse-reflectance studies, and a 4-mm o.d. quartz sidearm, for EPR studies. The sample was degassed typically for 4 h at 25 °C and then for 20 h at 180 °C (pressure 4×10^{-4} torr). The samples prepared for the Mössbauer study were degassed at 200 °C to 5×10^{-4} torr. For one EPR study a sample was degassed at 300 °C for 4 h, and the results showed that the higher degassing temperature did not significantly alter the spectrum. Following spectroscopic examination the samples were exposed to about 400 torr Cl_2 (Matheson) for 13 h at 25 °C. Excess Cl_2 was then removed from the light gray-blue zeolite by evacuation at 25 °C for 3 h (pressure = 7×10^{-5} torr).

The $[Fe^{II}(bpy)_3]$-Y(13) zeolite was treated in the same manner as the $[Fe^{II}(bpy)_3]$-Y(5.3) samples except that the temperature was maintained at 50 °C during the exposure to chlorine. In addition, the sample prepared for the Mössbauer study was treated with only 20 torr Cl_2 for 5 h.

X-ray Diffraction and Spectroscopic Methods. X-ray diffraction (XRD) patterns were recorded with a Seifert-Scintag PAD II diffractometer using Ni-filtered Cu radiation. The samples were allowed to equilibrate with atmospheric moisture for at least 24 h prior to recording their patterns.

X-Band EPR spectra were obtained with a Varian E-6S spectrometer. Samples were allowed to thermally equilibrate for at least

(1) Texas A&M University.
(2) University of Antwerp (U.I.A.).
(3) Peigneur, P.; Lunsford, J. H.; DeWilde, W.; Schoonheydt, R. A. *J. Phys. Chem.* **1977**, *81*, 1179.
(4) DeWilde, W.; Peeters, G.; Lunsford, J. H. *J. Phys. Chem.* **1980**, *84*, 2306.
(5) Quayle, W. H.; Lunsford, J. H. *Inorg. Chem.* **1982**, *21*, 97.
(6) Breck, D. W. "Zeolite Molecular Sieves"; Wiley: New York, 1974.
(7) Delgass, W. N.; Garten, R. L.; Boudart, M. *J. Chem. Phys.* **1969**, *50*, 4603.

0020-1669/82/1321-2226$01.25/0

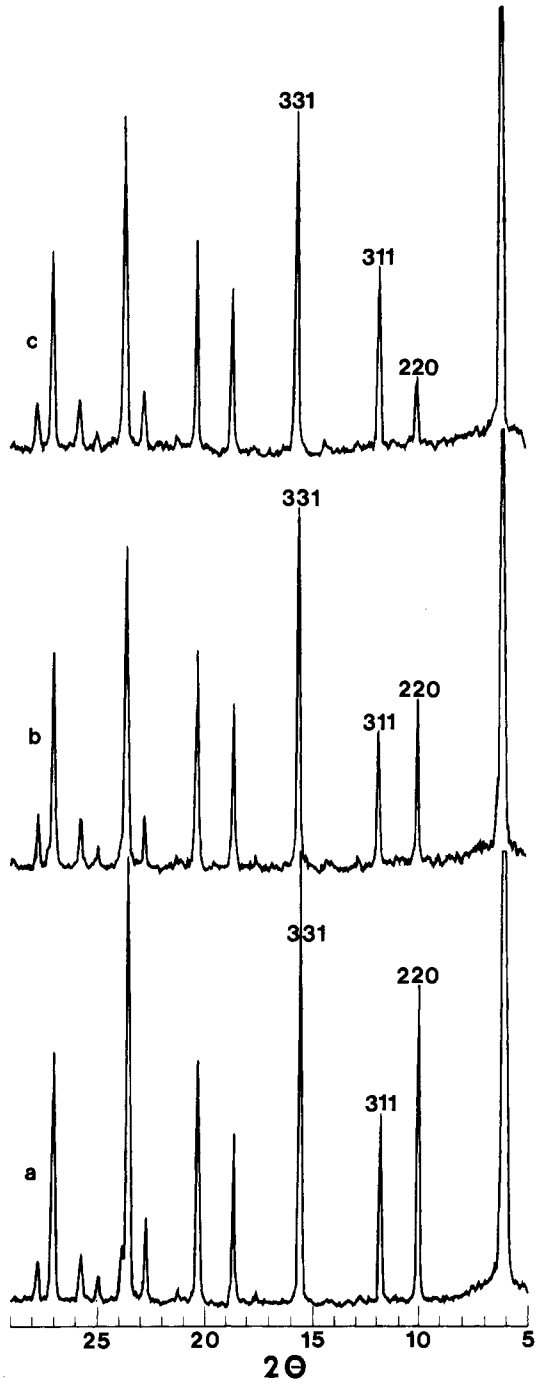

Figure 1. X-ray powder diffraction patterns of (a) Na–Y, (b) impregnated $[Fe^{II}(bpy)_3]$–Y and (c) $[Fe^{II}(bpy)_3]$–Y(5.3).

45 min at −196 °C prior to recording the spectra. The g values were calculated relative to a DPPH standard.

Visible-region (320–800 nm) diffuse-reflectance spectra were recorded with a Cary 14 spectrophotometer equipped with a type II diffuse-reflectance attachment. The logarithms of the Schuster–Kubelka–Munk remission functions were calculated by the equation $\log (F(R_\infty)) = \log [(1 - 10^{-A'})^2/(2 \times 10^{-A'})]$, where $A' = (A_{sample} - A_{ref})$. In the latter equation the A values, obtained directly from the spectrometer, may be related to the reflectance (R_∞) by $\log R_\infty = -A$. A Na–Y sample was used as the secondary reference. Absorber concentrations (C) were related to $\log (F(R_\infty))$ values at given wavelengths by $\log (F(R_\infty)) = \log C +$ constant, assuming no other species absorb at that wavelength and that the extinction coefficient at that wavelength remains constant over the concentration range of interest.

Mössbauer spectra were recorded with a Canberra Quanta automated spectrometer. The source consisted of approximately 5 mCi of ^{57}Co in Pd as prepared by New England Nuclear Corp. All data

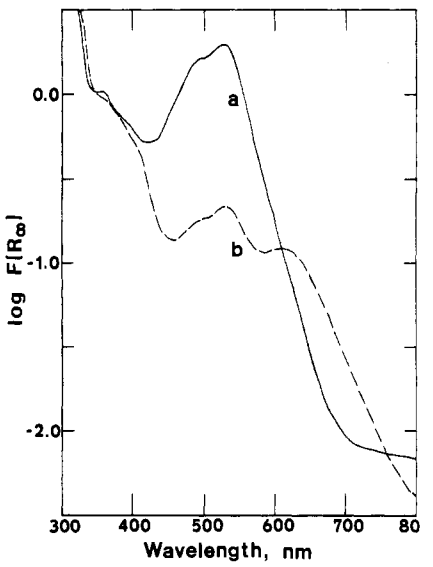

Figure 2. Visible-region diffuse-reflectance spectra of (a) $[Fe^{II}(bpy)_3]$–Y(5.3) and (b) $[Fe^{III}(bpy)_3]$–Y(5.3).

were obtained with the source and the absorber at room temperature. The spectrometer was calibrated with an iron foil and sodium nitroprusside dihydrate. Isomeric shift data are expressed relative to the nitroprusside standard. The zeolite samples (approximately 200 mg) were pressed (6 tons/cm^2) in 2-cm^2 disks. Spectra were collected until the statistical count rate error became less than 2% of the absorption peak height. The spectra were analyzed by a least-squares fit to a Lorentzian line shape.[8]

Results and Discussion

We previously reported that the location of large, transition-metal complexes either within or on the external surfaces of faujasite-type zeolites can be determined from an analysis of the XRD pattern.[5] An empirically derived relationship exists between the relative peak intensities of the 331, 311, and 220 reflections and the location of small cations. Cations are randomly distributed within the lattice if $I_{331} > I_{220} > I_{311}$, but if $I_{331} > I_{311} > I_{220}$, the cations assume positions at sites II and I′. Portions of the XRD patterns for samples of (a) Na–Y, (b) impregnated $[Fe^{II}(bpy)_3]$–Y, and (c) $[Fe^{II}(bpy)_3]$–Y(5.3) used in this study are reproduced in Figure 1. From a comparison of patterns a and b, it may be seen that little change occurred in the relative intensities of the 331, 311, and 220 peaks upon impregnation of Na-Y with $[Fe^{II}(bpy)_3]^{2+}$. We conclude that the zeolite lattice retained its originally random sodium ion distribution after impregnation. In contrast, analysis of the pattern for the $[Fe^{II}(bpy)_3]$–Y(5.3) sample indicated that significant cation redistribution occurred following complex formation within the zeolite supercages. The displacement of the sodium ions by the large $[Fe^{II}(bpy)_3]^{2+}$ complexes probably occurred in about one out of every 1.5 supercages for the sample containing 5.3 Fe ions per unit cell.

$[Fe^{II}(bpy)_3]$–Y(5.3). The visible-region diffuse-reflectance spectrum of the degassed $[Fe^{II}(bpy)_3]$–Y(5.3) sample is displayed in Figure 2, curve a. The reddish pink sample exhibits an absorption maximum at 528 nm. This can be compared with a literature value of $\lambda_{max} = 522$ nm for the $[Fe^{II}(bpy)_3]^{2+}$ complex in aqueous solution.[9] The zeolite-supported material also exhibits bands at 495, 386, and 353 nm. Busch and Bailar[10] observed the 522-nm band with a violet side shoulder as well as a 348-nm band for $[Fe^{II}(bpy)_3](ClO_4)_2$.

(8) Nullens, H.; DeRoy, G.; Van Espen, P.; Vansant, E. F.; Adams, F. *Anal. Chim. Acta* **1980**, *122*, 373.
(9) Ford-Smith, M. H.; Sutin, N. *J. Am. Chem. Soc.* **1961**, *83*, 1830.
(10) Busch, D. H.; Bailer, J. C., Jr. *J. Chem. Soc.* **1956**, 1137.

Table I. Mössbauer Hyperfine Parameters

sample	doublet	IS,[a] mm/s	QS,[c] mm/s	peak width, mm/s	% abund	anisotropy,[b] nm
$[Fe^{II}(bpy)_3]$-Y(5.3)	1	0.626 (4)	0.339 (4)	0.322 (8)	88 (2)	0.05 (3)
	2	0.74 (1)	1.25 (3)	0.35 (1)	12 (2)	
$[Fe^{II}(bpy)_3]$-Y(13)	1	0.455 (3)	0.354 (3)	0.307 (5)	55 (2)	0.03 (2)
	2	0.499 (6)	1.267 (8)	0.484 (9)	33 (2)	−0.07 (2)
	3	0.72 (2)	2.57 (3)	0.46 (1)	12 (2)	
$[Fe^{III}(bpy)_3]$-Y(13)	1	0.455 (3)	0.353 (5)	0.324 (7)	37 (2)	0.02 (2)
	2	0.546 (7)	1.232 (9)	0.483 (9)	29 (2)	−0.07 (2)
	3	0.69 (1)	2.57 (1)	0.47 (1)	11 (2)	
	4	0.208 (6)	1.68 (1)	0.358 (8)	22 (2)	

[a] Isomeric shift vs. nitroprusside. [b] The root of the difference of the mean-squared vibrational amplitudes parallel and perpendicular to the symmetry axis of the complex (see ref 13). [c] Quadrupole splitting.

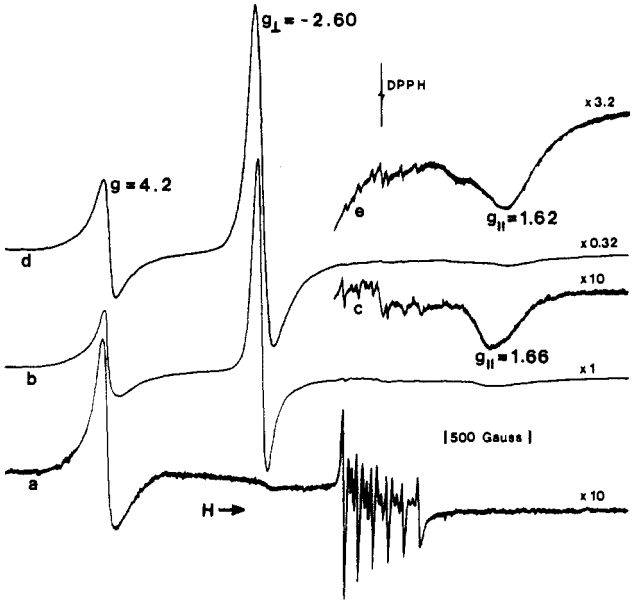

Figure 3. Electron paramagnetic resonance spectra taken at −196 °C of (a) $[Fe^{II}(bpy)_3]$-Y(5.3), (b) $[Fe^{III}(bpy)_3]$-Y(5.3), (c) b, at 10× greater receiver gain, (d) $[Fe^{III}(bpy)_3]$-Y(13) and (e) d, at 10× greater receiver gain.

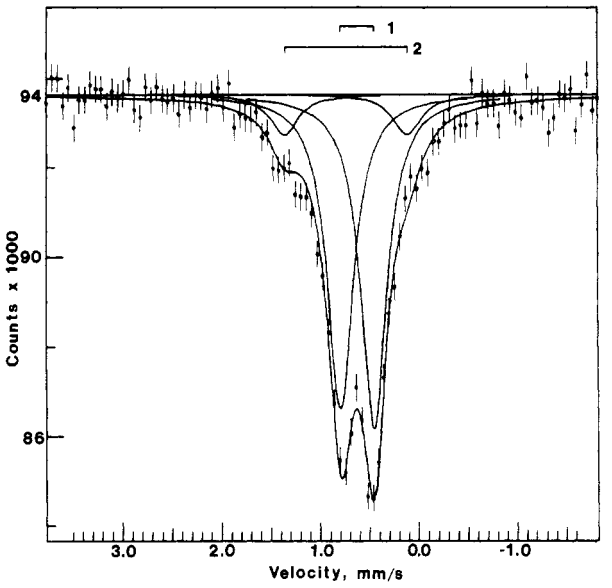

Figure 4. Mössbauer spectrum of $[Fe^{II}(bpy)_3]$-Y(5.3) with doublet parameters as in Table I.

The EPR spectrum of the sample is shown in curve a of Figure 3. The resonance at $g = 4.2$ may be attributed to tetrahedrally coordinated high-spin Fe^{3+} ions, an impurity which normally substitutes in Si and Al structural lattice sites.[11] Manganese(II), which is another impurity in the zeolite, gives rise to an sextet near $g = 2.0$.

Two iron doublets can be distinguished from the Mössbauer spectrum in Figure 4. The parameters are listed in Table I. Doublet assignments are based on commonly occurring parameters found in Mössbauer texts.[12,13] Doublet 1 may be assigned to low-spin Fe(II) in an octahedral environment, which probably arises from the $[Fe^{II}(bpy)_3]^{2+}$ complex situated near the center of the large cavity. The quadrupole splitting (QS) value of 0.339 mm/s compares favorably with a frozen aqueous solution value of 0.33 mm/s for $[Fe^{II}(bpy)_3]Cl_2$.[14] Our isomer shift (IS) value of 0.626 mm/s is larger than the literature[14,15] value of 0.46 mm/s. We attribute this difference to the change in environment which the complex would experience upon substitution of a zeolite lattice as a counterion for the ClO_4^- or Cl^- ions in frozen solution.[14,15] The polarizable bpy ligands might be influenced by a higher electron density within the zeolite lattice, resulting in a larger isomeric shift. The small peak width of the doublet (0.322 mm/s) in comparison to the source line width (0.28 mm/s) is indicative of a well-defined coordination geometry around the iron atoms which is slightly distorted from the ideal octahedral symmetry by a 0.05 nm lengthening along a C_2 axis.

The second, less intense, doublet in Figure 4 can be interpreted in two ways. It can be assigned either as a high-spin Fe(III) species in an octahedral environment or as a low-spin Fe(II) species. Although the IS value is rather high for a low-spin Fe(II) species, it might arise from a coordination number greater than 6. The QS value of 1.25 mm/s would support this supposition. In view of subsequent discussion we suggest that doublet 2 represents a low-spin Fe(II) moiety which resides inside the hexagonal prism of the zeolite lattice. In that location it would coordinate directly to six O(3) atoms. The high-spin Fe(III) characterized by the EPR spectrum of Figure 3a probably was not present in sufficient concentrations to be detected in the Mössbauer spectrum. It would appear from the relative abundances of the two sets of doublets in Table I that the reaction of bpy with Fe^{II}–Y is about 88% complete.

$[Fe^{III}(bpy)_3]$-Y(5.3). Oxidation of the degassed $[Fe^{II}(bpy)_3]$-Y(5.3) sample by chlorine gas produced a light gray-blue material. The visible diffuse-reflectance spectrum of the degassed material is displayed in Figure 2, curve b. This spectrum exhibits absorption maxima at 612, 527, and 494 nm, with a broad shoulder at about 360 nm on a larger band in the UV region. The 527- and 494-nm bands are due to unoxidized $[Fe^{II}(bpy)_3]^{2+}$ complexes. The literature value of

(11) Wichterlová, B.; Jirů, P. *React. Kinet. Catal. Lett.* **1980**, *13*, 197.
(12) Bancroft, G. M. "Mössbauer Spectroscopy. An Introduction for Inorganic Chemists and Geochemists"; McGraw-Hill: London, 1973.
(13) Gütlich, P.; Link, R.; Trautwein, A. "Mössbauer Spectroscopy and Transition Metal Chemistry"; Springer-Verlag: New York, 1978.
(14) Vértes, A.; Korecz, L.; Burger, K.; "Mössbauer Spectroscopy"; Elsevier: Amsterdam, 1979; p 282.
(15) Epstein, L. M. *J. Chem. Phys.* **1964**, *40*, 435.

Table II. EPR Data for Fe(III) Complexes

	$[Fe^{III}(bpy)_3]$-Y(5.3)	$[Fe^{III}(bpy)_3]$-Y(13)	$[Fe^{III}(bpy)_3](PF_6)_3$[a]
$g_\perp$	−2.60 ± 0.02	−2.60 ± 0.02	−2.61 ± 0.02
$g_\parallel$	1.66 ± 0.01	1.62 ± 0.01	1.61 ± 0.01
k	1.10 ± 0.05[b]	1.06 ± 0.05	1.07 ± 0.05
ν/ξ	3.27 ± 0.07[b]	3.07 ± 0.07	3.03 ± 0.07

[a] Data from ref 17. [b] Error limits on k and ν/ξ values are intended to represent value ranges obtained from calculations using the given g value error limits.

617 nm for the $[Fe^{III}(bpy)_3]^{3+}$ ion in concentrated H_2SO_4[9] may be compared with our value of 612 nm in the Y zeolite.

An estimate of the extent of the $[Fe^{II}(bpy)_3]^{2+}$ oxidation may be obtained since the logarithms of the diffuse-reflectance remission functions, log $(F(R_\infty))$, may be taken as directly proportional to the logarithms of the concentrations of absorbing species at individual wavelengths for these materials.[16] If $[Fe^{II}(bpy)_3]^{2+}$ was the only absorber at 527 nm, an 89% loss in Fe(II) concentration is calculated. Since the 612-nm band of the Fe(III) product may slightly overlap the 527-nm band of the reactant (see Figure 2b), the percent conversion to $[Fe^{III}(bpy)_3]^{3+}$ may well be somewhat greater than the calculated 89%. It should be noted that the intensity of the 612-nm band is not expected to be large for the Fe(III) complex in the zeolite since the values for the extinction coefficients of the tris(bipyridine)iron(II) complexes and -(III) complexes in solution are 8650 and 320 M^{-1} cm^{-1}, respectively.[9]

The EPR spectrum of the oxidized $[Fe^{III}(bpy)_3]$-Y(5.3) sample is presented in curves b and c of Figure 3. The experimentally determined $g_\perp$ and $g_\parallel$ values of −2.60 ± 0.02 and 1.66 ± 0.01, respectively, for the axially symmetric t_{2g}^5 $[Fe^{III}(bpy)_3]^{3+}$ complex in the zeolite compare favorably with literature values of $g_\perp = -2.61 \pm 0.02$ and $g_\parallel = 1.61 \pm 0.01$ for $[Fe^{III}(bpy)_3](PF_6)_3$ doped in a powdered, diamagnetic host.[17] Curve c of Figure 3 highlights the weak, broad $g_\parallel$ absorption at higher receiver gain. We infer from the absence of additional resonances in the g = 3.0–1.0 region that the reaction of Fe(II) with bpy in the zeolite is greater than 95% specific for tris(bipyridine) complexes over bis or mono complexes. The bis or mono complexes would give rise to different spectra since, as pointed out by DeSimone,[18] the low-spin d^5 configuration is a good probe of molecular structure and bonding. The observed g values vary widely and are sensitive to small changes in structure and to the covalent interaction with the ligands of the complex. For example, $[Fe^{III}(bpy)_2(CN)_2]^+$ exhibits values of $g_1 = 2.74$, $g_2 = 2.47$, and $g_3 = 1.54$.[19]

For comparison with literature results,[17] values of the orbital reduction factor, k, and the trigonal splitting factor, ν/ξ, were calculated from the equations of Bleany and O'Brien,[20] where $g_\parallel = 2[\sin^2\theta - (1 + k)\cos^2\theta]$, $g_\perp = -2[2^{1/2}k \cos\theta \sin\theta + \sin^2\theta]$, $\tan 2\theta = 2^{1/2}/(0.5\nu/\xi)$, and $0 < 2\theta < \pi$. The calculated values of ν/ξ and k listed in Table II are larger for the $[Fe^{III}(bpy)_3]$-Y(5.3) sample than values reported by De Simone and Drago[17] for $[Fe^{III}(bpy)_3](PF_6)_3$. Larger ν/ξ and k values in a zeolite system were also observed in our related study which compared $[Ru^{III}(bpy)_3]$-Y with $[Ru^{III}(bpy)_3](PF_6)_3$.[5] In that study we suggest that the trivalent complex within the zeolite supercage possibly encountered a higher negative charge density than in the doped powder sample. Distortion of the complex along a C_2 axis within the zeolite supercage would result in a change in the $g_\parallel$ value for the trivalent complexes.

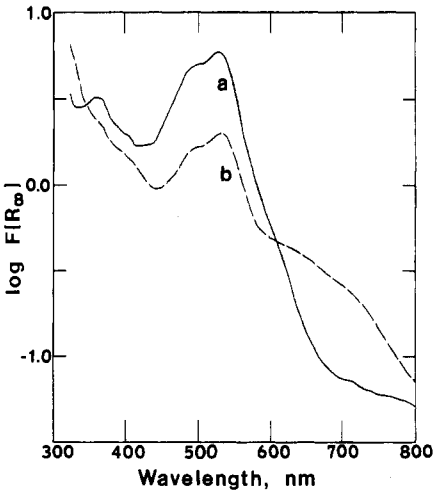

Figure 5. Visible-region diffuse-reflectance spectra of (a) $[Fe^{II}(bpy)_3]$-Y(13) and (b) $[Fe^{III}(bpy)_3]$-Y(13).

The resonance at g = 4.2 in the EPR spectrum of Figure 3b is noticeably more intense than that of the unoxidized $[Fe^{II}(bpy)_3]$-Y(5.3) sample as shown in Figure 3a. This increase in intensity may arise partially from additional Fe^{III} ions which would be produced from chlorine oxidation of the uncomplexed Fe^{II} ions in the $[Fe^{II}(bpy)_3]$-Y(5.3) sample.

From a comparison of the peak heights of the EPR spectra of Figure 3b, the Mössbauer doublet abundances of Figure 4 (Table I) and the extent of Fe(II) complex loss calculated from the diffuse-reflectance data, the apparent iron composition in the $[Fe^{II}(bpy)_3]$-Y(5.3) and $[Fe^{III}(bpy)_3]$-Y(5.3) samples may be estimated. For approximately 100 parts of iron, the $[Fe^{II}(bpy)_3]$-Y(5.3) sample contains about 88 parts divalent tris(bipyridine) complex, about 10 parts Fe(II) ion, and about 2 parts lattice bound and/or indeterminate Fe^{3+} ions. The $[Fe^{III}(bpy)_3]$-Y(5.3) sample contains about 73 parts trivalent tris(bipyridine) complexes, about 10 parts divalent complex, and about 17 parts Fe(III) uncomplexes and/or Fe(II) ion. The fact that there is no evidence for mono- or bis(bipyridine) complexes despite the apparent excess of iron in these samples should not be surprising in view of the reported stability constants for Fe(II)–bpy complexes in solution where log K_1 = 4.3, log K_2 = 3.7, and log K_3 = 9.5.[21] Moreover, the stability of the tris complexes within the zeolite supercages may well be enhanced over solution or crystalline phase formulations. Basolo and Dwyer,[22] for example, prepared the iron(II) bis(bipyridine) and mono(bipyridine) complexes by heating the tris complex for prolonged periods (30 h) at 100-150 °C in vacuo. The enhanced stability of other transition-metal complexes in mineral supported environments is now well documented.[23]

$[Fe^{II}(bpy)_3]$-Y(13). The visible-region diffuse-reflectance spectrum of degassed $[Fe^{II}(bpy)_3]$-Y(13) is shown in Figure 5a. This spectrum exhibits an absorption maximum at 526 nm as expected for a $[Fe^{II}(bpy)_3]^{2+}$ complex. Other bands are also observed at 494, 399, and 358 nm. Comparison of the log $(F(R_\infty))$ values at 527 nm for the 1.7 and 4.0 wt % Fe samples indicates tht the higher loading sample should contain about 2.9 times more tris(bipyridine) complex. The

(16) Delgass, W. N.; Haller, G. L.; Kellerman, R.; Lunsford, J. H. "Spectroscopy in Heterogeneous Catalysis"; Academic Press: New York, 1979; p 101.
(17) DeSimone, R. E.; Drago, R. S. *J. Am. Chem. Soc.* **1970**, *92*, 2343.
(18) DeSimone, R. E. *J. Am. Chem. Soc.* **1973**, *95*, 6238.
(19) Reiff, W. M.; DeSimone, R. E. *Inorg. Chem.* **1973**, *12*, 1793.
(20) Bleany, B.; O'Brien, M. C. M. *Proc. Phys. Soc., London, Sect. B* **1956**, *69*, 1215.
(21) McWhinnie, W. R.; Miller, J. D. *Adv. Inorg. Chem. Radiochem.* **1969**, *12*, 135.
(22) Basolo, F.; Dwyer, F. P. *J. Am. Chem. Soc.* **1954**, *76*, 1454.
(23) Maes, A.; Peigneur, P.; Cremers, A. *J. Chem. Soc., Faraday Trans. 1* **1978**, *74*, 182.

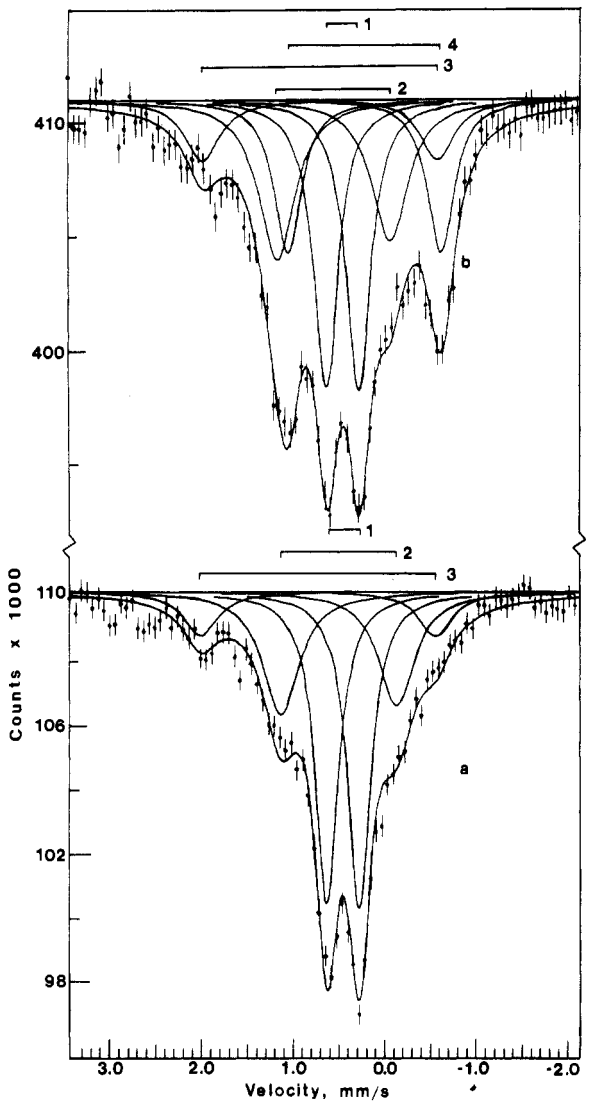

Figure 6. Mössbauer spectra of (a) $[Fe^{II}(bpy)_3]$–Y(13) and (b) $[Fe^{III}(bpy)_3]$–Y(13) with doublet parameters as in Table I.

EPR spectrum of $[Fe^{II}(bpy)_3]$–Y(13) exhibited the $g = 4.2$ resonance at somewhat greater intensity than was observed for $[Fe^{II}(bpy)_3]$–Y(5.3).

Three different iron doublets were observed in the Mössbauer spectrum of Figure 6a. The parameters are listed in Table I. Doublet 1 can be assigned to a low-spin Fe(II) species in octahedral coordination to three bpy ligands. The 55% abundance corresponds to a loading of about seven of those complexes per unit cell, and we therefore suggest that they exist near the center of each supercage. The low IS of this complex compared to the $[Fe^{II}(bpy)_3]$–Y(5.3) sample may be due to weakening of the Fe–bpy bond by interactions with other Fe species in the neighborhood. A slight lengthening along the C_2 axis of approximately 0.03 nm is indicated from our anisotropy calculations.

Doublet 2, Figure 6a, can be ascribed to a low-spin Fe(II) species in a distorted octahedral environment shortened along a C_2 axis by about 0.07 nm. Nearly every large cavity contains a bulky $[Fe^{II}(bpy)_3]^{2+}$ complex, so doublet 2 cannot be attributed to an independent entity in the large cavity. As calculated from the 33% abundance, one of these low-spin Fe(II) species should occur for every two supercages. We suggest that this moiety could be a low-spin Fe(II) π complex which would be located in the 12-membered oxygen ring at site IV (for site nomenclature, see ref 6). It could be π bonded to three rings from each of the $[Fe^{II}(bpy)_3]^{2+}$ complexes residing in the two supercages on either side of the 12-membered ring, as depicted in Figure 7. This coordination is consistent with the observed Mössbauer parameters. The IS would be higher than that for the $[Fe^{II}(bpy)_3]^{2+}$ complex because of the influence of π bonding on the d-orbital filling. The QS is consistent with a rather high distortion from the ideal octahedral symmetry. The large peak width can be understood in view of the various ways in which the π complex could be formed, i.e., whether or not the coordinating rings originate from the same or from different bpy ligands.

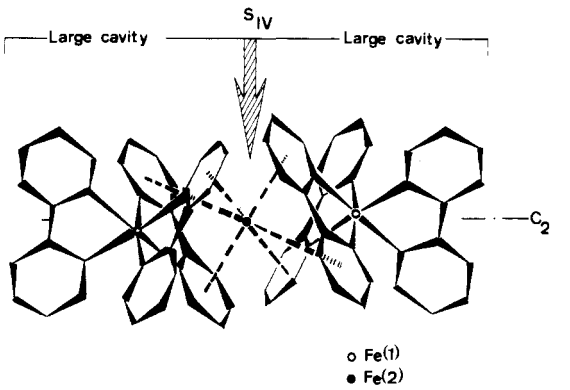

Figure 7. Depiction of proposed low-spin Fe(II) moiety located at site IV and π bonded to the ligands of two tris(bipyridine) complexes.

The parameters for doublet 3, Figure 6a, can be attributed to uncomplexed, high-spin Fe(III) in a very asymmetric environment. There should be two of these per unit cell based on the abundance of the doublet. It is difficult to determine the coordination number and consequently the cation site, but because of the large QS value, the location of these high-spin Fe(III) ions in the hexagonal prisms of the zeolite can be excluded.

$[Fe^{III}(bpy)_3]$–Y(13). A gray-pink sample was obtained following oxidation of $[Fe^{II}(bpy)_3]$–Y(13) by chlorine gas. The incomplete oxidation of the Fe(II) complex is immediately apparent from a comparison of the visible-region diffuse-reflectance spectra of the unoxidized (Figure 5a) and oxidized (Figure 5b) samples. The loss in $[Fe^{II}(bpy)_3]^{2+}$ complex concentration calculated from the log $(F(R_\infty))$ values at 526 nm was only 34% for the high-loading sample. Compared with the 612-nm $[Fe^{III}(bpy)_3]^{3+}$ band observed for the low-loading sample, the 612-nm band in Figure 5b is considerably broader. Loss of one or more bipyridine ligands might be expected to shift the Fe(III) band to the violet since conjugated electron-donor groups would be removed from the metal ion.[10] A mixture of tris-, bis-, and/or mono(bipyridine)iron(III) complexes would then produce a broad, featureless band at higher wavelength, but in view of the EPR and Mössbauer data presented below, we prefer an explanation which involves perturbation of the electronic states of the tris(bipyridine)-iron(III) complexes through π bonding of the bpy ligands to the unoxidized Fe(II) ions implicated above for the $[Fe^{II}(bpy)_3]$–Y sample

With the assumption of axial symmetry, the $g_\perp$ and $g_\parallel$ values for the $[Fe^{III}(bpy)_3]^{3+}$ complex in the high-loading sample taken from the EPR spectrum of Figure 3, curves d and e, are -2.60 ± 0.02 and 1.62 ± 0.01, respectively. As shown in Table II, the calculated k and ν/ξ values more closely resemble those of the doped powder $[Fe^{III}(bpy)_3](PF_6)_3$ sample. The distortion of the resonance near $g = 1.74$ in Figure 3e would appear to be anomalous because this feature was not reproduced in a second experiment with an outgassing temperature of 300 °C.

Four sets of iron doublets can be distiguished in the Mössbauer spectrum of the $[Fe^{III}(bpy)_3]$–Y(13) sample, as shown in Figure 6b. Parameters for doublet 1, listed in Table

I, are nearly identical with those observed for doublet 1 of the unoxidized sample. It is due to the $[Fe^{II}(bpy)_3]^{3+}$ complex located in the center of the zeolite supercages. Parameters for doublet 2 are also comparable to those of doublet 2, Figure 6a, and are again assigned to low-spin iron(II) species. Since the abundance of this doublet has not changed following Cl_2 treatment, within the uncertainty limits, it appears that these species are not available for oxidation. Indeed, the Fe(II) ions of the π-type complex proposed for the unoxidized sample should not be accessible to Cl_2 because they would be shielded by both of the complexes on either side of the 12-membered ring. Doublet 3 is also relatively unchanged following oxidation and remains assigned to an uncomplexed, high-spin Fe(III) species.

Doublet 4 of Figure 6b exhibits new parameters (Table I), and a low-spin iron(III) tris(bipyridine) complex is assumed to be responsible for it. The very small IS of this species as well as the large QS value is characteristic of low-spin Fe(II).[12] The sum of the abundance of doublets 1 and 4 agrees fairly well with the amount of tris(bipyridine) complex in the original $[Fe^{II}(bpy)_3]$–Y(13) sample. A chlorine oxidation efficiency of 33% is calculated from their abundance in agreement with the 34% value calculated from the diffuse-reflectance data. We assume that the trivalent iron complex experiences perturbations, possibly through π bonding of its bipyridine ligands to the doublet 2 Fe(II) ion, in much the same way as its divalent counterpart. Comparison of the EPR data (Table II) for the high- and low-loading trivalent complex tends to confirm this assumption.

Conclusions

Stable tris(2,2′-bipyridine)iron(II) complexes may be synthesized selectively upon exposure of Fe^{II}–Y zeolites to the ligand at 200 °C. The reaction is most effective at iron loadings less than that necessary for formation of one complex per lattice supercage. The zeolite environment appears to exhibit a higher degree of negative charge density than that of aqueous solution phases or doped powder matrices. Any excess, uncomplexed Fe(II) in the zeolite is forced from the supercage by the bulky bipyridine complex. At higher loadings the excess Fe(II) may possibly form π-type complexes with the bipyridine ligands of the tris complex, perhaps bridging two such complexes in adjacent supercages. This proposed dual function for the bpy ligands should reduce their interaction with the central iron atom of the tris complex.

At lower loadings chlorine gas oxidizes the divalent tris(bipyridine) complex with close to 90% efficiency. Since only partial oxidation is observed at higher loadings, it appears that either diffusion of the chlorine to the excess Fe(II) is inhibited or perhaps there is no space for the formation of chlorine ions at the oxidation sites. The iron(III) complexes also appear to be influenced by the higher negative charge density within the zeolite as compared to a doped powder sample.

Acknowledgment. The financial support of this work through NSF Grant CHE-7706792 and NFWO—Belgium is gratefully acknowledged.

Registry No. $[Fe^{II}(bpy)_3]^{2+}$, 15025-74-8; $[Fe^{III}(bpy)_3]^{3+}$, 18661-69-3.

Contribution from the Department of Chemistry, City University of New York, Queens College, Flushing, New York 11367

Resonance Raman Spectra of Ruthenium(II) Complexes of Bipyridine and Substituted Bipyridines: Ground- and Excited-State Properties

AMITABHA BASU, HARRY D. GAFNEY, and THOMAS C. STREKAS*

Received May 21, 1981

Resonance-enhanced Raman vibrational spectra are reported for $Ru(bpy)_3^{2+}$ and trissubstituted complexes of bipyridine substituted at the ring 4-position, $Ru(4\text{-}Xbpy)_3^{n+}$: X = NO_2, OEt (n = 2); X = PEt_3^+ (n = 5). For comparison, spectra of $Ru(bpy)_2Cl_2$, $Ru(4,4'\text{-}Me_2bpy)_3^{2+}$, and $Ru(4,4'\text{-}(NO_2)_2bpy)_2Cl_2$ are presented and analyzed. Analysis of the resonance Raman spectra for this series provides evidence for the nature of the bipyridine ring substituent effects on the electronic properties of the complexes. The ground-state properties are perturbed as shown by frequency shifts and the appearance of additional resonance-enhanced Raman bands. In addition, the variation in the relative intensities of the resonance-enhanced Raman bands can be related to the polarization of the excited state for the metal to ligand charge-transfer bands in resonance due to electronic effects of the substituents.

Introduction

Considerable recent interest has arisen concerning the photochemical properties of trissubstituted metal complexes of 2,2′-bipyridine and various derivatives,[1-4] particularly for ruthenium(II) and its analogues iron(II) and osmium(II). Of particular interest are the unusual excited-state redox properties of such species, which have been employed[5,6] in various photochemical systems to generate molecular hydrogen.

Numerous studies of the electronic absorption and emission spectra of the $M(bpy)_3^{2+}$ complexes (M = Fe, Ru, Os) have appeared,[7-10] and the assignment of the principal visible absorption bands as metal (t_2) to ligand (π^*) charge transfer in origin is generally accepted, although more detailed assignments[11] have recently been presented.

Resonance-enhanced Raman vibrational spectra are diagnostic of the nature of electronic transitions,[12,13] since they reveal the normal modes most intimately coupled to the electronic transition in resonance. Resonance-enhanced Raman vibrational spectra of $Ru(bpy)_3^{2+}$ have been reported,[14] as well as time-resolved resonance Raman spectra (RRS) of

(1) Meyer, T. J. *Acc. Chem. Res.* **1978**, *11*, 94.
(2) Sutin, N.; Creutz, C. *Adv. Chem. Ser.* **1978**, *No. 169*, 1.
(3) Weiner, M.; Basu, A. *Inorg. Chem.* **1980**, *19*, 2797.
(4) Fabian, R. H.; Klassen, D. M.; Sonntag, R. W. *Inorg. Chem.* **1980**, *19*, 1977.
(5) Kiwi, J. Borgarello, E.; Pelizzetti, E.; Visca, M.; Gratzel, M. *Angew. Chem., Int. Ed. Engl.* **1980**, *19*, 646.
(6) Giro, G.; Casalbore, G.; Dimarco, P. G. *Chem. Phys. Lett.* **1980**, *71*, 476.
(7) Day, P.; Sanders, N. J. *J. Chem. Soc. A* **1967**, 1536.
(8) Palmer, R. A.; Piper, T. S. *Inorg. Chem.* **1966**, *5*, 864.
(9) Hipps, K. W.; Crosby, G. A. *J. Am. Chem. Soc.* **1975**, *97*, 7042.
(10) Bryant, G. M.; Ferguson, J. E.; Powell, H. J. K. *Aust. J. Chem.* **1971**, *24*, 257.
(11) Felix, F.; Ferguson, J. E.; Gudel, H. U.; Ludi, A. *J. Am. Chem. Soc.* **1980**, *102*, 4096.
(12) Clark, R. J. H.; Stewart, B. *Struct. Bonding (Berlin)* **1979**, *36*, 1.
(13) Nishimura, Y.; Hirakawa, A. Y.; Tsuboi, M. *Adv. Infrared Raman Spectrosc.* **1979**, *5*.
(14) Bradley, P. G.; Kress, N.; Hornberger, B. A.; Dallinger, R. F.; Woodruff, W. H. *J. Am. Chem. Soc.* **1981**, *103*, 7441.

0020-1669/82/1321-2231$01.25/0